

Microstructural characteristics and microwave dielectric properties of Ba[Mg_{1/3}(Nb_{*x*/4}Ta_{(4-*x*)/4})_{2/3}]O₃ ceramics

Chen-Fu Lin^a, Horng-Hwa Lu^b, Tien-I. Chang^a, Jow-Lay Huang^{a,*}

^a Department of Materials Science and Engineering, National Cheng-Kung University, No. 1, Ta-Hsueh Road, Tainan 701, Taiwan, ROC

^b Department of Mechanical Engineering, National Chin-Yi Institute of Technology, Taichung 411, Taiwan, ROC

Received 17 May 2005; received in revised form 13 June 2005; accepted 17 June 2005

Available online 27 July 2005

Abstract

Sintering behaviors and microstructural characteristics in solid solutions of Ba[Mg_{1/3}(Nb_{*x*/4}Ta_{(4-*x*)/4})_{2/3}]O₃ (BMN_{*x*}Ta_{4-*x*}, *x* = 0, 1, 2, 3 and 4) were investigated by X-ray diffraction, SEM and TEM. Microwave dielectric properties, such as the relative permittivity (ϵ_r), quality factor (Q) value and temperature coefficient of resonator frequency (τ_f), were also measured. The excellent microwave dielectric property of Ba(Mg_{1/3}Ta_{2/3})O₃ (BMT) sample imply the necessity to sinter at higher temperature (1650 °C) and to use longer soaking times (9 h), but not for Ba(Mg_{1/3}Ta_{2/3})O₃ (BMN). The 1:2 B-site ordering was maintained at all Nb substitution contents and the 1:2 B-site ordering existed in the grains with antiphase domain boundaries (APBs). The Ba[Mg_{1/3}(Nb_{1/4}Ta_{3/4})_{2/3}]O₃ specimen exhibited excellent microwave dielectric properties, $\epsilon_r = 25.534$, $Qf = 140\,666$ GHz, and $\tau_f = 4.8$ (ppm/°C). The excellent microwave dielectric property is due to the improvement of sintering property by appropriate Nb atoms substitution in the BMT matrix and the maintaining of 1:2 ordering in the BMN_{*x*}Ta_{4-*x*} series. © 2005 Elsevier B.V. All rights reserved.

Keywords: Microwave dielectric; Microstructure

1. Introduction

The demands for microwave dielectric resonators are rapidly rising as communication systems depend more and more on microwave technology. The three key requirements for a dielectric resonator are a high relative permittivity (ϵ_r) for possible miniaturization (because the size of a dielectric resonator $\propto 1/\epsilon_r^{1/2}$), a high unloaded quality factor (Q) for a stable resonant frequency, and a near-zero temperature coefficient of frequency (τ_f) for temperature stable circuits. A complex perovskite ceramic A(B_{1/3}B'_{2/3})O₃, which was first reported by Kawashima et al. [1], is known to be excellent for the dielectric resonator and is used widely. One of the most important factors for improving the unloaded Q of the perovskite A(B_{1/3}B'_{2/3})O₃ ceramics is the ordering of B-site in A(B_{1/3}B'_{2/3})O₃ [2,3]. The Q value increases with the B-site ordering. The τ_f of a microwave dielectric can be controlled

in accordance with the volume mixture rule of the existing phases.

One of the superior microwave dielectrics is the complex perovskite ceramic Ba(Mg_{1/3}Ta_{2/3})O₃, which has a high unloaded quality factor ($Qf = 300\,000$ GHz), high dielectric constant ($\epsilon_r = 25$), and small TCF (< 5 ppm/°C). Although this material has excellent microwave dielectric properties, the high sintering temperature (1600–1650 °C) and long soaking time [4] (~50 h) due to low sinterability of Ba and Ta atoms is a problem. Barium magnesium niobate, Ba(Mg_{1/3}Nb_{2/3})O₃ (BMN), a complex perovskite compound is known to possess high $\epsilon_r (= 32)$ and Q value ($Qf = 56\,000$ GHz) [5]. However, BMN has relative positive τ_f compared with that of other complex perovskite. Except for the similar crystal structure between BMN and BMT, the Nb⁵⁺ and Ta⁵⁺ ions also have a similar ionic radius (radius of Nb⁵⁺ and Ta⁵⁺ ions are 0.69 and 0.68 Å). The Ba[Mg_{1/3}(Nb_{*x*/4}Ta_{(4-*x*)/4})_{2/3}]O₃ microwave ceramic were initially investigated by Thirumal et al. [6] and Janaswamy et al. [7]. The authors paid attention to the preliminary dielectric properties and crystal

* Corresponding author. Tel.: +886 6 234 8188; fax: +886 6 276 3586.
E-mail address: JLH888@mail.ncku.edu.tw (J.-L. Huang).

structure. However the relative investigation on the ordering structure was deficient. The main purpose of this study includes two parts: (1) the crystal structure, microstructure, the degree of B-site ordering and the microwave dielectric properties of the BMT and BMN at various sintering conditions are investigated; (2) the properties of microstructures $\text{Ba}[\text{Mg}_{1/3}(\text{Nb}_{x/4}\text{Ta}_{(4-x)/4})_{2/3}]\text{O}_3$ (simplified as $\text{BMN}_x\text{T}_{4-x}$) with various Nb substitution content are also discussed.

2. Experimental procedure

$\text{Ba}[\text{Mg}_{1/3}(\text{Nb}_{x/4}\text{Ta}_{(4-x)/4})_{2/3}]\text{O}_3$ ($\text{BMN}_x\text{T}_{4-x}$, $x=0, 1, 2, 3$ and 4) were synthesized using a conventional solid-state reaction method from individual oxide and carbonate powders: barium carbonate (BaCO_3 , Nippon Chemical Industrial Co., Ltd., 99.85%), magnesium oxide (MgO , Fluka, 99.8%), niobium oxide (Nb_2O_5 , Alfa Aesar, 99.9%) and tantalum oxide (Ta_2O_5 , Strem Chemicals, 99.8%). The materials were weighed in the appropriate molar ratio and mixed by grinding with ZrO_2 balls in the ethanol media for 24 h. The slurry was dried in a rotary evaporator (Heidolph 2011, Germany). After grinding and sieving with 100 mesh, the powders were calcined at 1100°C for 3 h in air. The calcined powders were mixed and ground with the PVA binder additive in Al_2O_3 mortar and then sieved with 45 mesh. The mixed powders were uniaxially pressed into pellets under the pressure of 100 MPa with 9 mm in diameter and 5 mm in height. The pellets were then cold isostatic pressed (CIP) at the pressure of 200 MPa. The pellets were sintered at $1600\text{--}1650^\circ\text{C}$ for 6–9 h in air.

The bulk densities of sintered specimens were measured by the Archimedes method. The crystal structures of sintered samples were analyzed by X-ray diffractometer (Rigaku D/max-IV, Japan). The microstructures of samples were observed by scanning electron microscopy (SEM, Philips XL-40PEG, Holland). The samples were polished to $1\ \mu\text{m}$, thermally etched at 1400°C for 30 min, and coated with Pt before SEM examination. The more detail microstructure and crystal structure of sintered samples were analyzed by transmission electron microscopy (TEM, JEOL 3010, USA). Thin foils for the TEM investigations were prepared by mechanically grinding the ceramic pellets to a thickness of $20\text{--}30\ \mu\text{m}$. The samples were mounted on copper aperture grids, and a final thinning was conducted via argon-ion milling (Gatan Model 600 Dual Ion Mill, CA).

To treat the B-site ordering quantitatively, an ordering factor S is defined as follows [8,9]: $S = \sqrt{\frac{(I_{100}/I_{110,102})_{\text{obs}}}{(I_{100}/I_{110,102})_{\text{order}}}}$ where $(I_{100}/I_{110,102})_{\text{obs}}$ is the ratio of the observed intensities of the superlattice reflection (100) from (110) and (102) of the XRD patterns. For a completely ordered BMT and BMN structure, the intensity ratio of $(I_{100}/I_{110,102})_{\text{order}}$ are calculated to be 8.3/100 and 3.16/100.

The relative permittivity ϵ_r and Q value were measured using a TE_{011} resonator frequency peak by placing the sample in a metal cavity. The τ_f was measured using the Hakki and Coleman method [10]. The τ_f was obtained by measuring TE_{011} resonator frequency in the temperature range of $30\text{--}80^\circ\text{C}$. The relationship between τ_f and dielectric constant was represented by $\tau_f = -\alpha - \tau_e/2$, where α is the thermal expansion coefficient. In materials with the perovskite structure, the value of α maintained a constant value of $10\ \text{ppm}/^\circ\text{C}$ [11].

3. Results and discussion

3.1. Sintering behaviors of $\text{Ba}(\text{Mg}_{1/3}\text{Ta}_{2/3})\text{O}_3$ (BMT) and $\text{Ba}(\text{Mg}_{1/3}\text{Nb}_{2/3})\text{O}_3$ (BMN) specimens

Fig. 1 shows X-ray analysis of BMT and BMN specimens sintered at various sintering conditions. BMT and BMN had similar X-ray diffraction patterns and the diffraction peaks all belonged to the same diffraction planes except for the two highest angle peaks $2\theta \cong 64.53^\circ$ and 73.28° . The peaks (100), (111), (200), (112) and (103) marked by asterisk indicated the superlattice reflection as mentioned by Ra and Phulé [12] and Hu et al. [13] and the superlattice reflections of BMT were obviously stronger than BMN. The X-ray results indicate that sintered BMT and BMN specimens have the same crystal structure and no apparent second phase are produced at various sintering conditions.

Table 1 shows the densities, the $(I_{100}/I_{110,102})_{\text{obs}}$ intensity ratios, ordering factor and microwave properties of BMT and BMN specimens at various sintering conditions. The relative density of sintered BMT and BMN specimens were higher than 98% (the theory density of BMT and BMN is 7.657 and $6.236\ \text{g}/\text{cm}^3$) [14] at various sintering conditions. From the X-ray data, the $(I_{100}/I_{110,102})_{\text{obs}}$ intensity ratios

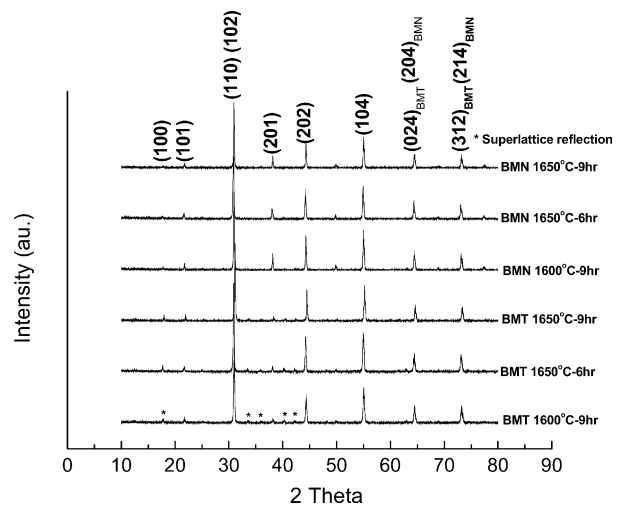


Fig. 1. X-ray diffraction patterns of BMT and BMN specimens sintered at various sintering conditions.

Table 1

The densities, the $(I_{100}/I_{110,102})_{\text{obs}}$ intensity ratios and microwave dielectric properties of BMT and BMN specimens at various sintering conditions

| | Density (g/cm ³) | $(I_{100}/I_{110,102})_{\text{obs}}$ | Ordering factor (S) | Dielectric constant(ϵ_r) | Qf value |
|-----------------|------------------------------|--------------------------------------|---------------------|-------------------------------------|--------------------|
| BMT 1600 °C–6 h | 7.5094 (98.07%) | 0.0542 | 0.808 | 24.469 | 49559 (8.242 GHz) |
| BMT 1650 °C–6 h | 7.6017 (99.28%) | 0.0618 | 0.863 | 24.748 | 70958 (8.257 GHz) |
| BMT 1650 °C–9 h | 7.5258 (98.29%) | 0.0698 | 0.917 | 24.451 | 100042 (8.166 GHz) |
| BMN 1600 °C–6 h | 6.1170 (98.09%) | 0.0306 | 0.984 | 31.602 | 83439 (7.286 GHz) |
| BMN 1650 °C–6 h | 6.1262 (98.24%) | 0.0303 | 0.979 | 31.771 | 85154 (7.183 GHz) |
| BMN 1650 °C–9 h | 6.1638 (98.84%) | 0.0286 | 0.951 | 31.932 | 92060 (7.27 GHz) |

of the BMT specimens increased from 0.0542 to 0.0698 with increasing sintering temperature and time, but slightly decreased from 0.0306 to 0.0286 for BMN specimens. The $(I_{100}/I_{110,102})_{\text{obs}}$ intensity ratios of BMT ceramics were apparently larger than those of BMN ceramics. By further precise calculation of ordering factor, it was indicated that the ordering factor of BMT ceramic was improved from 0.808 to 0.917 with increasing sintering temperature and soaking time, but the ordering factor of BMN ceramics were in the range 0.951–0.984 and not influenced obviously by sintering temperature and soaking time. On the contrary, the ordering degree of BMN ceramics was higher than which of BMT ceramics at the same sintering condition. As mentioned by Cullity and Stock [15], the intensity of X-ray diffraction are proportional to the atomic number, so the lower $(I_{100}/I_{110,102})_{\text{calc}}$ values of BMN ceramics (equal to 0.0316 [9]) compared to BMT ceramics (equal to 0.083 [8]) were contributed by the lower atomic number of Nb than Ta. The lower intensity ratio of $(I_{100}/I_{110,102})_{\text{obs}}$ for BMN ceramics compared to BMT ceramics could also explained by the lower atomic number of Nb. In the research of Hughes et al. [16], they also mentioned that the scattering powder difference between $\text{Zn}^{2+}/\text{Nb}^{5+}$ is lower than for $\text{Zn}^{2+}/\text{Ta}^{5+}$ due to the lower atomic number of niobium and results in the fact that the ordering in BZN based materials is more difficult to observe by X-ray diffraction than in BZT. The characteristic of the ordering factor for BMT at various sintering condition reveals that the BMT was difficult to sinter unless at elevated temperature and longer soaking time, but not for BMN.

The relative permittivity of BMT was in the range 24.451–24.748 and 31.602–31.932 for BMN at various sintering conditions. The relative permittivity increased with the sintering density. Kolodiazny et al. [17] reported that the dependence of the dielectric constant on the porosity of BMT ceramics obeys the Maxwell–Wagner relation [18]: $\epsilon' = \epsilon'_1 \left\{ 1 + \frac{3\gamma(\epsilon'_2 - \epsilon'_1)}{2\epsilon'_2 + \epsilon'_1} \right\}$ where $\epsilon'_1 = 25$ for completely dense BMT ceramics, ϵ'_1 is the permittivity of vacuum, and γ the porosity of ceramics. Since $\epsilon'_2 = \epsilon'_1$ is negative, the dielectric constant increases with the decrease in porosity. It was suggested that the enhancement of dielectric constants of BMT and BMN were due to the lower porosity with increasing sintering density.

The Qf value of BMT increased obviously from 49559 to 100 042 GHz at elevated sintering temperature and longer

soaking time. Nevertheless, the Qf value of BMN only slightly increased from 83 439 to 92 060 GHz at elevated sintering temperature and longer soaking time. The Qf value of BMT was improved doubly with elevated sintering temperature and longer soaking time. The Qf value of BMT was improved obviously due to the increase of the degree of ordering degree. Yoon et al. [19] reported that one of the most important factors for improving the quality factor of the complex perovskite $\text{A}(\text{B}_{1/3}\text{B}'_{2/3})\text{O}_3$ ceramics is the ordering of B-sites in $\text{A}(\text{B}_{1/3}\text{B}'_{2/3})\text{O}_3$. As the B-site ordering increases, the Qf value increases. The Qf value of BMN was approximate and only slightly improved due to small increase of the degree of ordering at elevated sintering temperature and longer soaking time. For reaching the excellent microwave dielectric property of BMT it is necessary to sinter at high temperature and long soaking time to overcome the sintering difficulty of Ta atom and to obtain the higher degree of B-site ordering. Comparing with Ta, Nb has a lower atomic number (Ta: 73, Nb: 41), so BMN can be easily sintered completely and has high a degree of B-site ordering.

3.2. $\text{Ba}[\text{Mg}_{1/3}(\text{Nb}_{x/4}\text{Ta}_{(4-x)/4})_{2/3}]\text{O}_3$ series ($\text{BMN}_x\text{T}_{1-x}$) with various Nb substitution contents

To understand the influences of Nb substitution for Ta in BMT, $\text{Ba}[\text{Mg}_{1/3}(\text{Nb}_{x/4}\text{Ta}_{(4-x)/4})_{2/3}]\text{O}_3$ ($\text{BMN}_x\text{T}_{4-x}$, $x = 0, 1, 2, 3,$ and 4) were synthesized by solid-state reactive method. The samples were sintered at 1650 °C for 9 h and then analyzed by X-ray diffraction, SEM, TEM and microwave dielectric property.

Fig. 2 shows the X-ray diffraction analysis of BMNT series which were sintered at 1650 °C for 9 h. The results indicate that the BMNT have the same crystal structure with different amount Nb substitution and no apparent secondary phase is produced due to the similar ion radii between Nb and Ta (radius of Nb^{5+} and Ta^{5+} are 0.69 and 0.68 Å) and the same crystal structure (as showed in Fig. 1). However, the intensity of superlattice diffraction peaks was lowered by the Nb substitution. Fig. 3 shows the $(I_{100}/I_{110,102})_{\text{obs}}$ intensity ratios of BMNT serious calculated from the X-ray diffraction patterns (Fig. 2) at various Nb substitution contents. The intensity ratio decreased from 0.06977 (BMT, $x = 0$) to 0.02864 (BMN, $x = 4$). In the $\text{Ba}(\text{Mg}_{1/3}\text{Nb}_{2/3})\text{O}_3$ – BaZrO_3 system [20] and the $\text{Ba}(\text{Mg}_{1/3}\text{Ta}_{2/3})\text{O}_3$ – BaSnO_3 system [21],

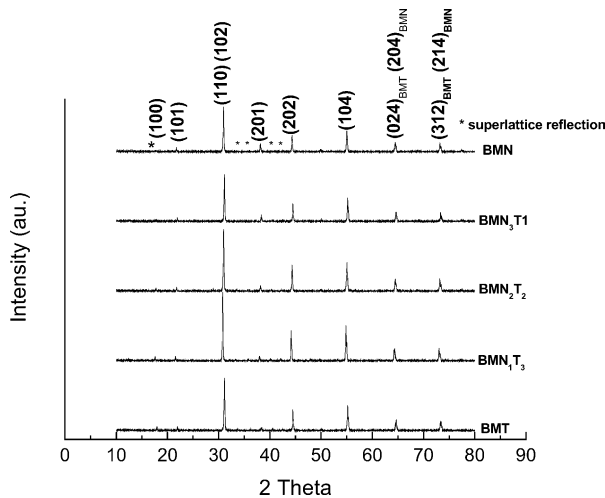


Fig. 2. X-ray diffraction patterns of BMNT series at various Nb substitution contents. The samples were sintered at 1650 °C for 9 h.

the substitution of Zr and Sn for Nb and Ta also resulted in a weaker intensity of superlattice diffraction peaks. As described in Fig. 1 and Table 1, the BMN specimens show lower $I_{100}/I_{110,102}$ ratio than BMT due to the lower atomic number of Nb, so the superlattice diffraction intensity of BMNT were lower with increasing the Nb substitution contents. But the ordering behavior of the B-site atom could not be described completely by the X-ray diffraction analysis. A more detailed analysis will be given later by TEM.

Fig. 4 shows the apparent and theoretical densities of the BMNT series at various Nb substitution contents. The theoretical densities were calculated by the mixing rule according to the molar ratio with $D_{\text{BMT}} = 7.657 \text{ g/cm}^3$ and $D_{\text{BMN}} = 6.236 \text{ g/cm}^3$ [14]. The apparent density of BMNT decreased from 7.53 g/cm^3 ($x=0$) to 6.16 g/cm^3 ($x=4$) with

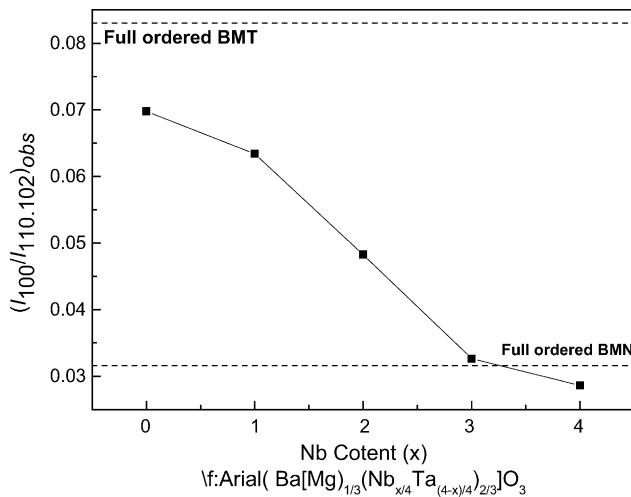


Fig. 3. The $(I_{100}/I_{110,102})_{\text{obs}}$ intensity ratios of BMNT series at various Nb substitution contents.

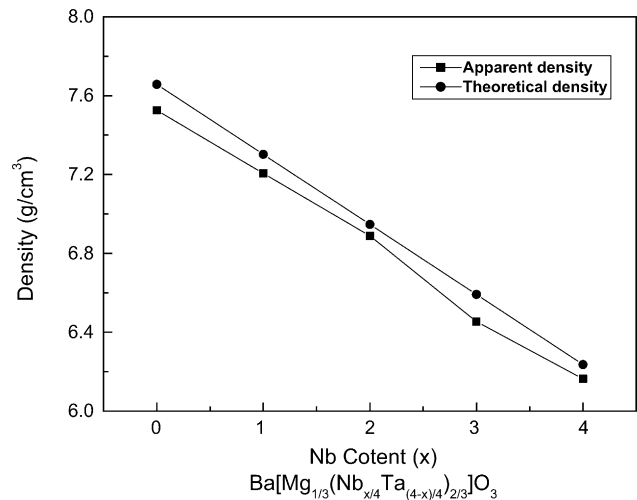


Fig. 4. Apparent and theoretical densities of BMNT series at various Nb substitution contents. The samples were sintered at 1650 °C for 9 h.

Nb substitution content and matched with the trend of the theoretical density. The results mean that the lighter Nb atoms were entirely replaced the heavier Ta atoms. As a result, the relative densities of BMNT were all larger than 98.

Fig. 5 shows the SEM micrographs and average grain sizes of BMNT series at various Nb substitution contents after thermal etching. The crystal grain structures of BMT and BMN both belonged to a round shape grain structure which consisted with big grains (3–4 μm) and small grains (<1 μm), but BMN displayed generally larger grain sizes than BMT. The larger grain size of BMN than BMT was due to the high mobility and the lower atomic number of Nb, so the grain growth of BMN could proceed easier than BMT in the sintering process. As the Ta atoms were replaced by Nb atoms ($x=1, 2, \text{ and } 3$), the microstructures were similar as BMT and BMN, but the grain size of the BMNT series was smaller than BMT and BMN for the big as well as for the small grains (Fig. 5(b)). The values of the average grain sizes of BMT (2.140 μm , Fig. 5(a)) and BMN (2.203 μm , Fig. 5(c)) were approximate, but the average grain size of BMN_2T_2 (1.563 μm , Fig. 5(b)) was obviously smaller than in BMT and BMN. In the sintering process, more nucleation sites in the initial stage, lower energy sintering condition (lower sintering temperature, shorter soaking time) and the appearance of second phase in grain growth stage also could result in the decrease of grain size. It is suggested that the smaller grain size of the BMNT series is due to an increase of the nucleation sites with Nb substitution.

Fig. 6 shows the [1 1 0] zone axis electron diffraction patterns of a BMN_1T_3 ($x=1$) specimen. The other Nb substitution contents ($x=2$ and 3) led to similar results. The pattern was indexed and based on the simple cubic perovskite unit cell for better understanding. The superlattice reflections of the 1:2 ordering are characterized by the presence of $\pm 1/3[1 1 1]$ -type reflections as indicated by arrows in Fig. 6. Kolodiazhnyi et al. [17] and Kim et al. [22] reported that the

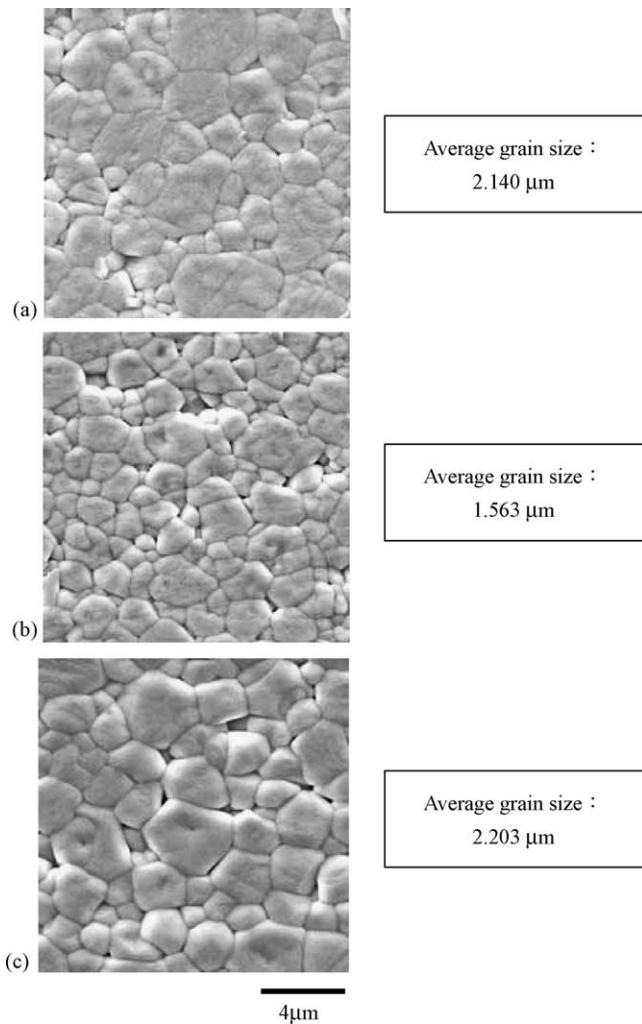


Fig. 5. The SEM micrographs of BMNT series at various Nb substitution contents after thermal etching. (a) BMT ($x=0$); (b) BMN_2T_2 ($x=2$); (c) BMN ($x=4$).

superlattice reflection of 1:2 ordering existed in BMT and BMN. When the Ta atoms were replaced by the Nb atoms, the 1:2 ordering could still be maintained in spite of the Nb substitution content.

In the previous researches of the $\text{Ba}(\text{Zn}_{1/3}\text{Ta}_{2/3})\text{O}_3\text{-BaZrO}_3$ [23] and $\text{Ba}(\text{Mg}_{1/3}\text{Nb}_{2/3})\text{O}_3\text{-BaZrO}_3$ [20] series ceramics, small BaZrO_3 substitution (~ 5 mol) could introduce an ordering transformation from 1:2 to 1:1 ordering. The ordering transformation was suggested to be related to the degeneracy of the quality factor. The maintenance of 1:2 ordering in BMNT series is suggested to be related with the similar ionic radii of the Nb and Ta atoms.

Fig. 7 shows the TEM micrographs of BMN_3T_1 . Antiphase domain boundaries (APBs) (indicated by arrowheads) were found in the grains of BMN_3T_1 specimens. The APBs were also formed in BMNT samples with other Nb substitution contents. The APBs are not confined crystallo-

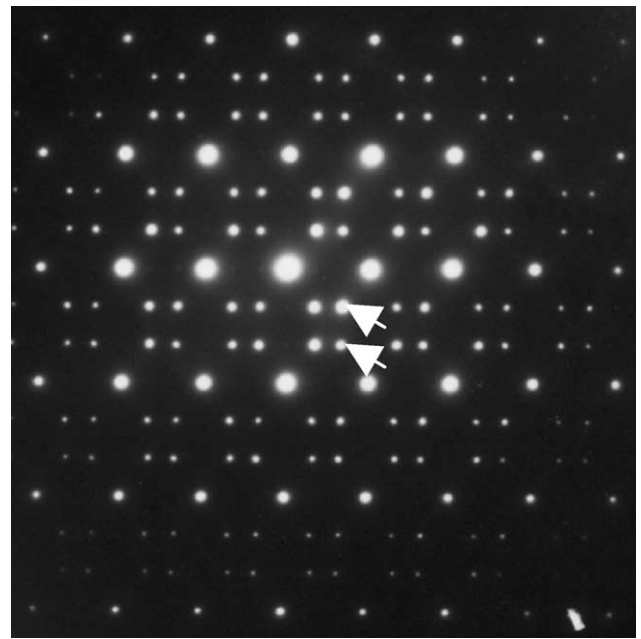


Fig. 6. [110] zone axis electron diffraction patterns of BMN_1T_3 ($x=1$) specimen.

graphically and normally they are characteristically curved. Moreover, the APBs are formed by the chemical ordering of B-site ions [24]. The APBs were also found in BMT [25] and BMN [26], and it was suggested that the grains with 1:2 ordering domains were separated by APBs. In a more detailed TEM research using selective area diffraction (SAD), it is evidenced the superlattice reflection of 1:2 ordering was mainly produced from the crystal grains with APBs.

The [110] zone axis electron diffraction patterns of BMN_3T_1 grains without APBs is shown in Fig. 8. The 1:2 superlattice reflection patterns disappear for grains without APBs, and the grains of BMNT with other Nb substitution contents also displayed similar results. For positions of the grains far away from the APBs, the 1:2 superlattice reflections were not produced in the [110] zone axis pattern. In the previous study of $\text{Ba}(\text{Zn}_{1/3}\text{Ta}_{2/3})\text{O}_3\text{-BaZrO}_3$ perovskite microwave dielectrics [23], the authors suggested that low losses of the 1:2 ceramics were derived from the stabilization of the ordering-induced domain boundaries (such as APBs) via a partial segregation of Zr cations. As a result, it was suggested that the existence of APBs is strongly related to the ordering in BMNT ceramics.

Fig. 9 shows the microwave dielectric properties of BMNT series with various Nb substitution content. The relative permittivity of BMNT (Fig. 9(a)) increased from 24.451 ($x=0$) to 31.932 ($x=4$) with Nb substitution contents, but the resonant frequency decreased from 8.166 to 7.270 GHz. The elevated relative permittivity of the BMNT series with increasing Nb substitution content is due to the formation of a $\text{Ba}[\text{Mg}_{1/3}(\text{Nb}_{x/4}\text{Ta}_{(4-x)/4})_{2/3}]\text{O}_3$ solid solution and also

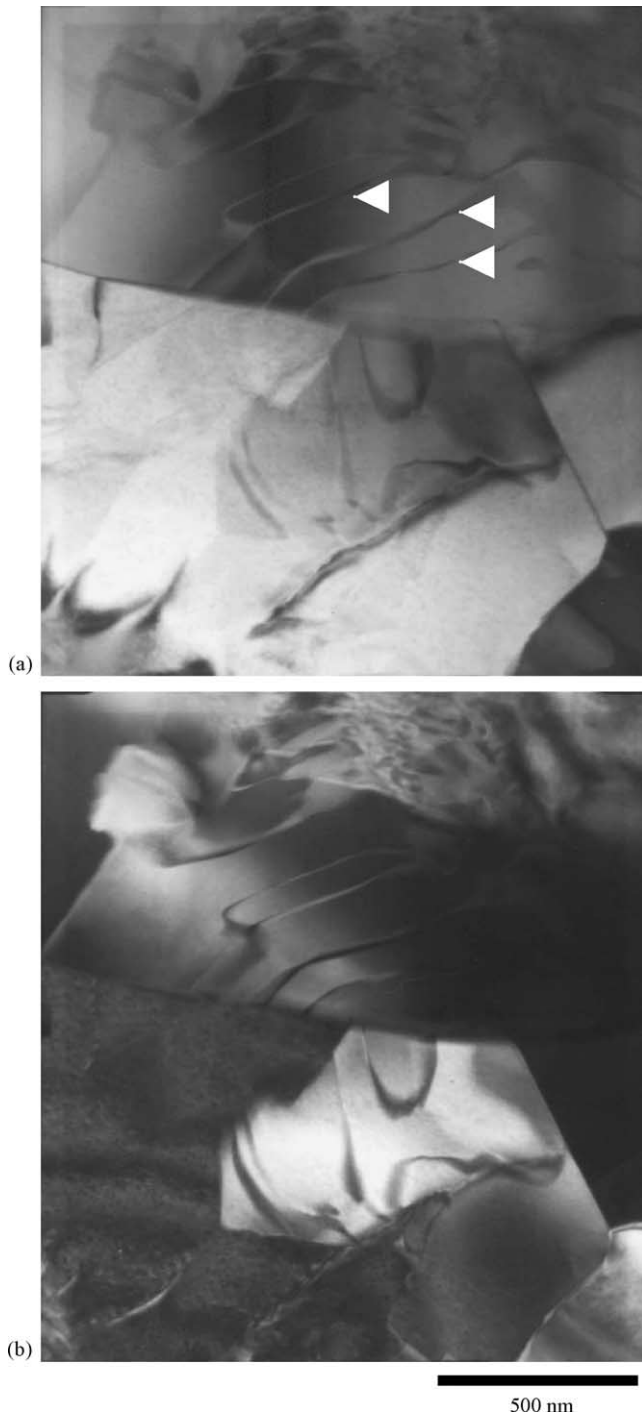


Fig. 7. TEM micrographs of BMN_3T_1 ($x=3$) sample illustrate the APB (indicated by arrowheads). (a) Bright field (BF); (b) dark field (DF).

indicated that the substitution of lower atomic number Nb can result in the increase of relative permittivity. In the previous research of $\text{BaNd}_{2(1-x)}\text{Sm}_{2x}\text{Ti}_5\text{O}_{14}$ microwave dielectric ceramics [27], the substitution of lower atomic number Nd atom also resulted in an elevated value of the dielectric constant. Higher electronic polarizability will cause higher values of ϵ_r as Nd occupies a site which will enhance

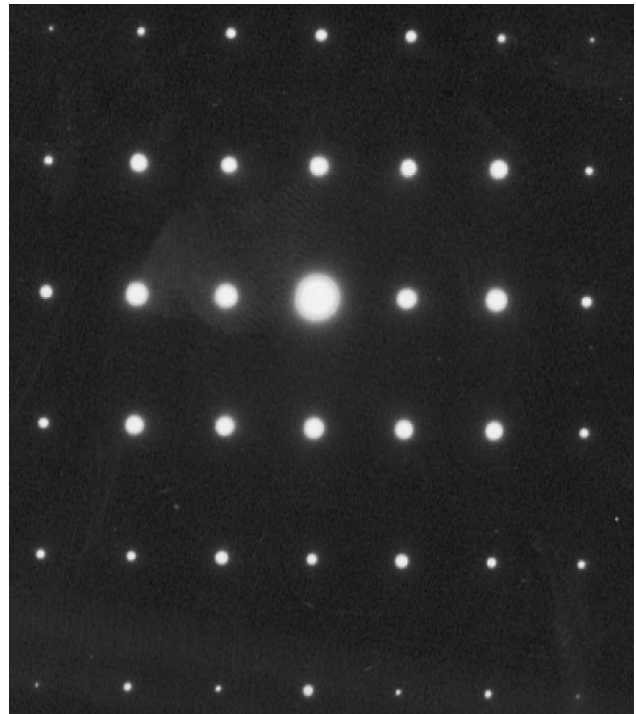


Fig. 8. [1 1 0] zone axis electron diffraction pattern of BMN_3T_1 ($x=3$) grain without APB.

the dielectric response of the system for a small increase in the electronic polarizability of the ion occupying the site.

The Qf value of the BMNT series increased from 99 963 GHz at $x=0$ to the maximum value 1 406 666 GHz at $x=1$ and then remained in the range between 92 060 and 109 756. It is suggested that the excellent Qf value at $x=1$ is due to the improvement of sintering property by appropriate Nb atom substitution in the BMT matrix. For $x=2-4$, the BMNT series could be seen as mainly a BMN matrix with Ta atom substitution. As shown in Table 1, the microwave dielectric properties of BMN were not affected by the elevated sintering temperature and long soaking time, so it is suggested that the Qf value of BMNT for the $x=2-4$ series could not be improved by Nb substitution. In lanthanum-substituted $\text{Ba}(\text{Mg}_{1/3}\text{Ta}_{2/3})\text{O}_3$ ceramics [28], both 1:2 and 1:1 ordered structure were formed and it was suggested that the increase-and-decrease behavior of the quality factor is attributed to a variation in the ordered structure. In the $\text{Ba}(\text{Zn}_{1/3}\text{Ta}_{2/3})\text{O}_3$ – BaZrO_3 solid solution, Davies et al. [23] presumed that the low losses of the 1:2 ordered ceramics were derived from the stabilization of the ordering-induced domain boundaries via the segregation of the Zr cations. In addition to the improvement of the sintering process and the maintenance of 1:2 ordering in the BMNT series, the stabilization of the ordering-induced domain boundaries via segregation of Nb cations was suggested to be the main factor that the BMN_1T_3 ceramics have better Qf value than the BMT and BMN ceramics.

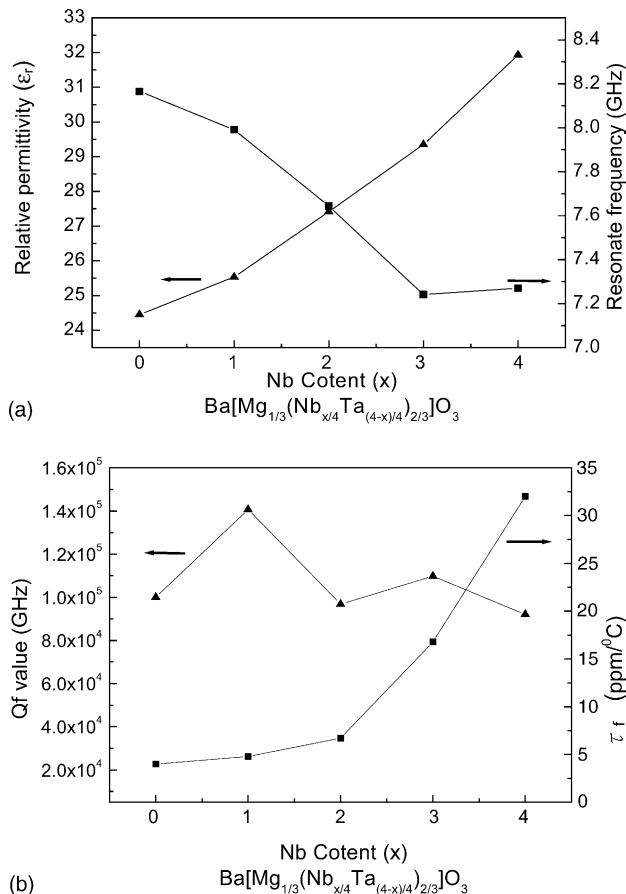


Fig. 9. The microwave properties of BMNT series at various Nb substitution content. (a) Dielectric constant and resonant frequency; (b) Qf value and temperature coefficient of resonant frequency.

The τ_f of BMNT series increased slowly from 4 ppm/°C ($x=0$) to 6.7 ppm/°C ($x=2$) and then drastically increased to 34 ppm/°C ($x=4$). The drastic increase τ_f of BMNT is contributed by the high τ_f value of the BMN matrix. For the $\text{BMN}_x\text{T}_{4-x}$ series at $x=1$, which exhibits excellent microwave dielectric properties, $\epsilon_r=25.534$, $Qf=140\,666$ GHz, and $\tau_f=4.8$ ppm/°C.

4. Conclusion

For BMT and BMN, reaching excellent microwave dielectric properties of BMT it is necessary to sinter at high temperature and to use long soaking times to overcome the sintering difficulty of Ta atoms. However, the microwave dielectric properties of BMN are not strongly affected by the sintering condition due to the lower atomic number Nb.

For the $\text{Ba}[\text{Mg}_{1/3}(\text{Nb}_{x/4}\text{Ta}_{(4-x)/4})_{2/3}]\text{O}_3$ series ($\text{BMN}_x\text{T}_{4-x}$), excellent solid solutions are formed at all Nb substitution contents ($x=0, 1, 2, 3$, and 4) due to the similar ionic radii of Ta and Nb. From SEM observation, smaller grain sizes of BMNT are formed with Nb substitution due

to heterogeneous nucleation. From TEM analysis, the 1:2 B-site ordering of BMNT series is maintained at all Nb substitution contents and the 1:2 B-site ordering mainly exists in the grain with APBs. For the $\text{BMN}_x\text{T}_{4-x}$ series at $x=1$, which exhibits excellent microwave dielectric properties, $\epsilon_r=25.534$, $Qf=140\,666$ GHz, and $\tau_f=4.8$ ppm/°C. It is suggested that the excellent microwave dielectric properties are due to the improvement during sintering by an appropriate Nb atom substitution in the BMT matrix, preservation of 1:2 ordering in the BMNT series and stabilization of the ordering-induced domain boundaries via the segregation of Nb cations.

Acknowledgment

The authors would like to thank National Science Council of the Republic of China for its financial support under the Contract No. NSC-92-2216-E-006-011.

References

- [1] S. Kawashima, M. Nishida, I. Ueda, H. Ouchi, Proceedings of First Meeting on Ferroelectric Materials and their Applications, Keihin Printing Co., Ltd., Kyoto, Japan, 1977, pp. 293–296.
- [2] S.B. Desu, H.M. O'Bryan, J. Am. Ceram. Soc. 68 (1985) 546–551.
- [3] E.S. Kim, K.H. Yoon, Ferroelectrics 133 (1992) 187–192.
- [4] J. Shimada, Eur. Ceram. Soc. 23 (2003) 2647–2651.
- [5] S. Nomura, Ferroelectrics 49 (1983) 61–70.
- [6] M. Thirumal, I.N. Jawahar, K.P. Surendiran, P. Mohanan, A.K. Ganguli, Mater. Res. Bull. 37 (2002) 2321–2334.
- [7] S. Janaswamy, G.S. Murthy, E.D. Dias, V.R.K. Murthy, Mater. Lett. 55 (2002) 414–419.
- [8] K. Matsumoto, T. Hiuga, K. Takada, H. Ichinura, Proceedings of the Sixth IEEE International Symposium on Applications of Ferroelectrics, American Ceramic Society, 1986, pp. 118–121.
- [9] A. Dias, V.S.T. Ciminelli, F.M. Matinaga, R.L. Moreira, J. Eur. Ceram. Soc. 21 (2001) 2739–2744.
- [10] B.W. Hakki, P.D. Coleman, IRE Trans. Microwave Theory Tech. MTT-8 (1960) 402–410.
- [11] E.L. Colla, I.M. Reaney, N. Setter, J. Appl. Phys. 74 (1993) 3414–3425.
- [12] Seung-Hyun Ra, Pradeep P. Phulé, J. Mater. Res. 14 (1999) 4259–4265.
- [13] X. Hu, X.-M. Chen, Y.J. Wu, Mater. Lett. 54 (2002) 279–283.
- [14] T. Kolodiaznyia, A. Petric, A. Belous, O. V'yunov, O. Yanchevskij, J. Mater. Res. 17 (2002) 3182–3189.
- [15] B.D. Cullity, S.R. Stock, Elements of X-ray Diffraction, 3rd ed., Prentice-Hall, Upper Saddle River, NJ, 2001, pp. 123–166.
- [16] H. Hughes, D.M. Iddies, I.M. Reaney, Appl. Phys. Lett. 79 (2001) 2952–2954.
- [17] T.V. Kolodiaznyia, A. Petrica, G.P. Joharia, A.G. Belousb, J. Eur. Ceram. Soc. 22 (2002) 2013–2021.
- [18] N.E. Hill, W.E. Vaughan, A.H. Price, M. Davies, Dielectric Properties and Molecular Behavior, Van Nostrand Reinhold Company, London, 1969, 283 pp.
- [19] Ki Hyun Yoon, Dong Pil Kim, Eung Soo Kim, J. Am. Ceram. Soc. 77 (1994) 1062–1066.
- [20] Mehmet A. Akbas, Peter K. Davies, J. Am. Ceram. Soc. 81 (1998) 670–676.
- [21] Lai-Cheng Tien, Chen-Chia Chou, Dah-Shyang Tsai, Ceram. Int. 26 (2000) 57–62.

- [22] Young-Woong Kim, Jae-Hwan Park, Jae-Gwan Park, J. Eur. Ceram. Soc. 24 (2004) 1775–1779.
- [23] Peter K. Davies, Jianzhu Tong, Taki Negas, J. Am. Ceram. Soc. 80 (1997) 1727–1740.
- [24] F. Galasso, J. Pyle, Inorg. Chem. 2 (1963) 482–484.
- [25] D.J. Barber, K.M. Moulding, Ji Zhou, Maoqiang Li, J. Mater. Sci. 32 (1997) 1531–1544.
- [26] Hwack Joo Lee, Hyun Min Park, Yang Koo Cho, Hyun Ryu, Yong Won Song, Jong Hoo Paik, Sahn Nahm, Jae-Dong Byun, J. Am. Ceram. Soc. 83 (1997) 2267–2272.
- [27] V. Satheesh, P. Murugavel, V.R.K. Murthy, B. Viswanathan, Mater. Sci. Eng. B 48 (1997) 202–204.
- [28] Lai-Cheng Tien, Chen-Chia Chou, Dah-Shyang Tsai, J. Am. Ceram. Soc. 83 (2000) 2074–2078.